*Preprints* (www.preprints.org) | NOT PEER-REVIEWED | Posted: 18 January 2021 doi:10.20944/preprints202101.0350.v1

# Non-Destructive Test to Diagnosing Wear of Marine Gas Turbine Blades

L.Y. Villagrán-Villegas[*1a], M. Patiño-Ortiz[2a], L. H. Hernández-Gómez[2b], J.C. Anzelmetti-Zaragoza[1b], J.A. Del Ángel-Ramos[1c], J.J. García-Mejía[3]

**Corresponding author*

1. Universidad Veracruzana, Facultad de Ingeniería Mecánica y Eléctrica. Prolongación Venustiano Carranza S/N, Col. Revolución 93390, Poza Rica, Veracruz, México.

2.- INSTITUTO POLITÉCNICO NACIONAL - Escuela Superior de Ingeniería Mecánica y Eléctrica - Sección de Estudios de Posgrado e Investigación Edificio 5. 2do Piso, Unidad Profesional Adolfo López Mateos "Zacatenco" Col. Lindavista, C.P. 07738, Ciudad de México, México.

3.- Instituto Tecnológico de Veracruz - Av. Miguel Ángel de Quevedo 2779, Col. Formando Hogar, 91897, Veracruz; Veracruz, México

Email:[1*]yvillagran@uv.mx,mpatino2002@ipn.mx[2a],luishector56@hotmail.com[2b],jesusgmejia@yahoo.com.mx[3]

**Abstract**

In this paper, a non-destructive test to diagnose wear of blade´s compressor of a gas turbine is reported. Gas turbine was operating in Campeche City, Mexico, in a very aggressive environment, where the entry of solid particles is unavoidable. The objective was to reduce cost of maintenance in this equipment. Analysis on a blade of gas turbine was performed, which was in operation on an offshore platform. Compressor blade was exposed to a severe damage by the impact of particles and environmental pollutants such as salts, sands and sulphurs.

In first stage of this analysis, a visual inspection with a borescope was performed, which has the ability to illuminate dark internal areas, with a bright light for visual examination and/or make a photographic reproduction in semi-annual maintenance cycles. Images analysis was used to determine the typical failure modes.

In a second stage, a tribological characterization was carried out. Chemical composition of the material of blades was obtained. Scanning electron microscopy (SEM) was used to measure roughness and evaluate degradation of surfaces of blades after 30,000 service hours.

The points, where peak stresses were calculated, correspond to those places in witch corrosion and some irregular scratches similar to plowing action, was observed. These are the points in which failures take place.
Results showed wear modes were originated by a severe stinging action. Also, large craters, similar to those observed in solid particle erosion, were developed by at normal impact.
In the same way it could be found some localized areas with a witch corrosion and irregular scratches similar to plowing action, was observed. These are the points in which failures take place.

**Keywords:** Gas turbine blades, Non-destructive testing, Borescope,Optical 3Dscanner.

## 1. Introduction

In oil and gas platforms, entry of solid particles (see Figure 1) in gas turbines is unavoidable [1]. The environment has a relatively passive role in the operation cycle of gas turbine; there are certain atmospheric conditions that can affect operation and life of gas turbines [2].

*Figure (1). Gas turbine inlet air.*

So, the selection of materials in their design plays an important role in achievement of a greater efficiency and a safer and more cost-effective operation. Metallurgical and mechanical points of view in most common faults of gas turbine's blades are considered. Lifespan of a blade is reduced due to operating environment and high mechanical and thermal stresses, where two or more factors typically act simultaneously [3]. Most common degradation mechanisms are: blade contamination and pitting, clearing between rotor and stator, and erosion of leading and trailing edge of blade of hot and cold part of gas turbine. Degradation is mainly caused by: inlays, corrosion, hot corrosion, oxidation, erosion, abrasion, particles melting and mechanical degradation. Research on turbine's blades starts with visual observations, optical microscopy, scanning electron microscopy, fractography analysis, metallography, structural analysis and hardness tests. In Centaur 40 gas turbine (see Figure 2), the most common degradation mechanisms are: air foil (blade) fouling and pitting (loss of flow profile caused by corrosion and surface deposits); opening of blade clearances and leading and trailing edge erosion (caused by mechanical solid and liquid impacts on rotor blades). Several mechanisms cause degradation of compressor blades, for example: fouling, corrosion, erosion, abrasion, particle fusing and mechanical degradation [4].

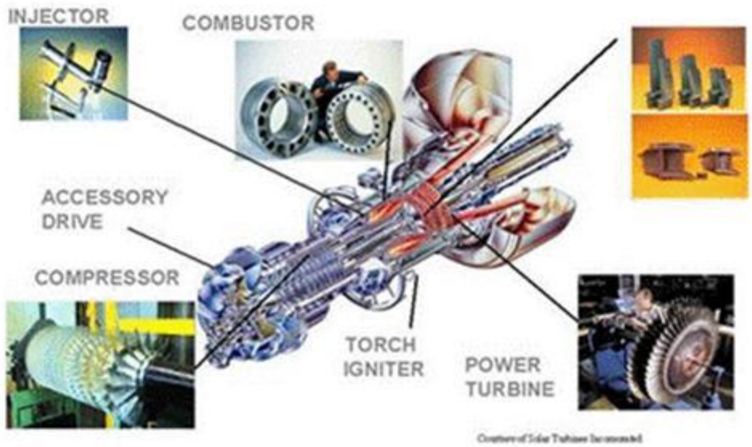


*Figure (2). C40 gas turbine. (by Solar Turbines)*

The most commonly used materials in gas turbine's blades are titanium or nickel super alloys and tungsten-molybdenum alloys; its assembly on rotor requires special care, paying special attention to optimum angle [5], some of the materials commonly used for manufacture of turbine's blades are martensitic stainless steels 403 or 403 Cb [6], with a chromium content of 12% (see Table 1).

*Table 1. Materials commonly used for manufacture of turbine's blades.*

| Grade | Chemical composition | Material |
|---|---|---|
| AISI 403 | Fe12Cr0.11C | Martensitic stainless steel. |
| AISI 403 + Cb | Fe12Cr0.2Cb0.15C | Martensitic stainless Steel add Nb |
| GTD-450 | Fe15.5Cr6.3Ni0.8Mo0.03C | Hardening by precipitation of stainless steel |

Preprints (www.preprints.org) | NOT PEER-REVIEWED | Posted: 18 January 2021 doi:10.20944/preprints202101.0350.v1

Blades operate at great vibratory forces, which requires sufficient resistance to fatigue; in particular, they must be manufactured with careful processes to support wear and resonance conditions, as well as to function optimally depending on pressure, temperature and viscosity conditions of fluid.

Axial compressor as the power turbine are formed by a certain number of stages, each stage involves a blade's disc, each blade of axial compressor in Centaur 40 gas turbine, inlet air gas turbine is room temperature (15 °C sea level) and increases its temperature when it is compressed, reaching 1,800 °C after passing through combustion chambers. Centaur 40 gas turbine consists of 11 stages in axial type air compressor, pressure ratio is 10.3: 1 and air flow inlet is 18.7 kg/sec (41.3 lb/sec). Variable blades begin to open when the Pcd (Pressure compressor discharge) reaches approximately 32 psi (gp) and fully open when Pcd reaches approximately 76.5 lb/in$^2$ (gauge) [7].


*Figure (3). 7th. Stage's blade, Rotor Axial Compressor.*

A study of wear damage of a seventh-stage's blade of axial compressor of a gas turbine (see Figure 3) was carried out. Manufacturer recommends routine maintenance at 30,000 hours to reduce chances for shutdown of gas turbine. In this study, the C40 gas turbine at 24,000 hours (shutdown) in field and out of service after 30,000 hours was analysed. This gas turbine was operating in Campeche City, Mexico (see Table 2), in a very aggressive environment, where entry of solid particles is unavoidable.

*Preprints* (www.preprints.org) | NOT PEER-REVIEWED | Posted: 18 January 2021 doi:10.20944/preprints202101.0350.v1

*Table 2. Operating condition of gas turbine in Campeche, Mexico.*

| | |
|---|---|
| **Northeast Marine Region Cantarell Nohoch ALFA** | • 30 units - 4700 H.P. ($11,474,303.12 US)-Cantarell<br>• 5 units 4700 H.P. – Nohoch Alfa<br>• Highly aggressive environment<br>• 8,000 Bd = $388,960.00 US – Nohoch-A |
| **Faults in gas turbine blades** $ 155,495 US **Reduce overhaul costs** | • Foreing Object Damage<br>• Mechanical<br>• Metalurgical<br>• Wear |
| **Mechanisms of degradation in materials** | • Inclusion<br>• Corrosion<br>• Erosion and abrasion<br>• Fusion of particles<br>• Mechanical degradation |
| **Analysis of wear $ 2,764.75 US** | • The set of blades in identical units and under similar operating conditions must accumulate at least 8 000 hours of operation without problems and no inspection. |

This paper proposes a methodology to carry out an analysis of damage caused by wear of axial compressor´s blades in a gas turbine.

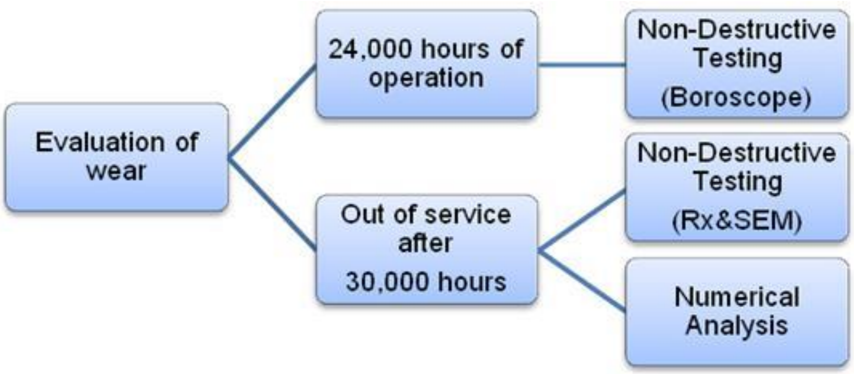


*Figure (4). Evaluation of wear.*

Work was developed in three stages. In first one, a thorough visual inspection of gas turbine's blade was carried out, an analysis of borescope images of surfaces of vanes was carried out in site, and second stage: microstructural tests were carried out on blade. In second stage, a sample to obtain chemical composition of material was analysed, and roughness to know surface degradation of the same was measured; Scanning Electron Microscopy (SEM) and Rx to identify wear mechanisms in several sample was used. Analysis on trailing edge was performed, leading edge and central part of blade.

Preprints (www.preprints.org) | NOT PEER-REVIEWED | Posted: 18 January 2021 doi:10.20944/preprints202101.0350.v1

## 2. Visual Examination

### 2.1 Borescope Analysis (24,000 hours).

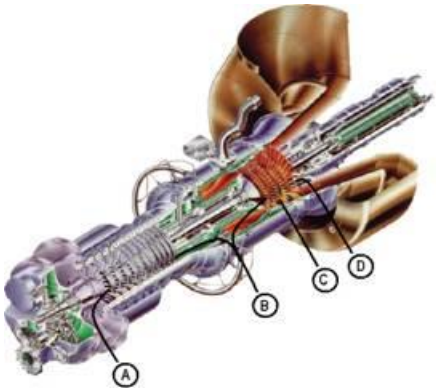


*Figure (5). Four ports where borescope can be introduced. (by Solar Turbines)*

Borescope test is a primary diagnostic method for turbo machinery maintenance; it is an inspection test that includes notification of the condition of equipment and effective programming of any necessary maintenance intervention. C40 gas turbine has four ports, where borescope can be introduced (Figure 5). Internal inspections are necessary to determine if wear or thermal erosion is present. Additionally, these inspections will take into account any damage caused by the impact of foreign objects (FOD), or if corrosion has occurred, and allow internal components to be assessed for thermal deterioration, fractures or distortion.

Corrosive attacks on aerodynamic surfaces can also be detected by borescope inspection.

A borescopic inspection verifies that:

• Damage is the result of a blade or nozzle being hit by an object that originates in first stages of gas turbine section and axial compressor or combustor.

• The area of impact damage is at or near the tip of blade and vibration is stable and does not exceed the limits. Then unit can be operated (until a replacement or a scheduled revision can be obtained) while is closely monitored. If damage of blade is between the root of blade and the middle of its body, regardless of level of vibration reached, the unit should not be restarted and should be checked. Corrosion on same parts of gas turbine's blade can be tolerated, however, if corrosion is evident at the tip of blade, the unit should be turned off and checked. If damage was the result of an object from within gas turbine stage (such as a turbine's blade portion or a nozzle surface), the unit should not be restarted.

Changes in dimensions of blade will affect natural frequency of the blades. The damage or loss of material that occurs at the tip of blade will increase natural frequency. If damage occurs at

 doi:10.20944/preprints202101.0350.v1

or near the root of blade, it weakens structurally and decreases its natural frequency. Natural frequencies of blades are above normal operating speed of a gas turbine. However, a reduction in natural frequency of blades could bring it closer to normal operating speed of the starter motor [8].

| **Access point** | **Photo** | **Description** | **Inspection** |
|---|---|---|---|
| Inlet air<br>**A1** | 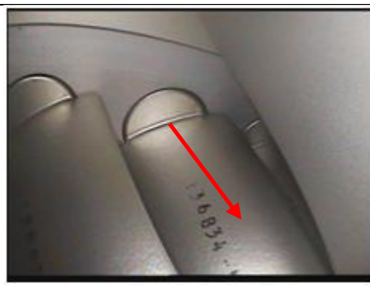 | First stage of variable inlet guide vanes (IGV) | Erosion, corrosion, pitting and impact for foreign object damage (F.O.D.) |
| Inlet air<br>**A2** | 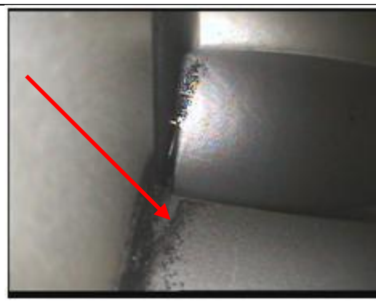 | First stage of compressor's blades. | Defected surface, corrosion, pitting and impact for foreign object damage (F.O.D.) |
| Inlet air<br>**A3** |  | Second stage of variable inlet guide vanes (IGV) | Defected surface, corrosion, pitting and impact for foreign object damage (F.O.D.) |
| Inlet air<br>**A4** | | Second stage of compressor blades. | Several dent and wear in tip blade. |

Preprints (www.preprints.org) | NOT PEER-REVIEWED | Posted: 18 January 2021 doi:10.20944/preprints202101.0350.v1

*Figure (6). Borescope test of C40 gas turbine (24,000 hours).*

In Borescope analysis, contamination in first stage of axial compressor was observed, it is a mixture of oil vapours that can prevent variable blades from opening or closing, which can lead to a low turbine performance and, even serious damage to turbines. The stage seventh of axial compressor has impregnated with dirt and debris, which is usually detergent and water used for washing of axial compressor's rotor (Figure 6), but this routine activity of maintenance is annual and technical engineer only carries out chemical analyses of water to detect metals in samples. In fact, his drag of solid particles by gas flow is another major problem during the operation of turbines. These foreign particles can either be deposited over turbine trail and blades (see Figure 1), causing wear and reducing efficiency of the turbine, or be launched at high velocities against blade surfaces, promoting formation of erosion pits in preferential areas, which can act as stress raisers [9–10].

## 2.2 Non-Destructive Test: Rx &SEM (30,000 hours)

A characterization of surface of physical and chemical materials requires selection of an appropriate group of analytical and methodological techniques [11].

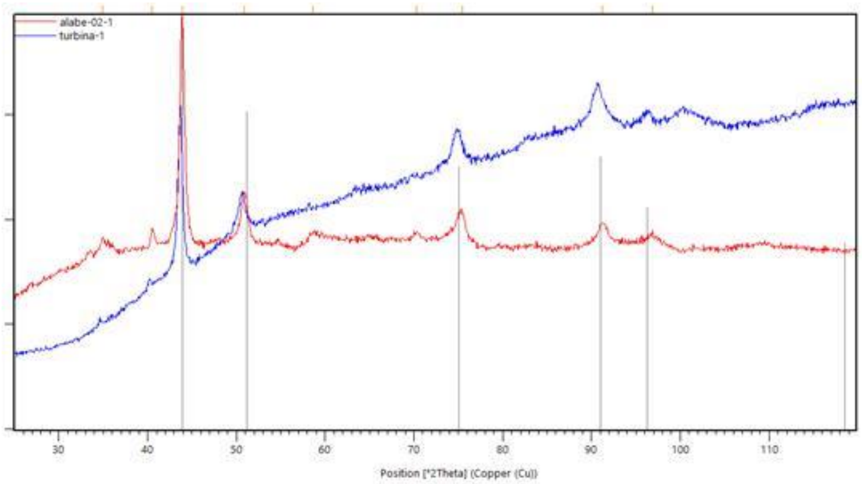


*Figure (7). Chemical compositions used EDS.*

Energy dispersive X-ray (EDS) to obtain chemical composition was used. Chromium, Iron, Nickel and Carbon were detected and obtain quantitative analysis by Atomic Absorption Spectroscopy: chromium 17.9%, nickel 11.4%, molybdenum 0.01% and silicon 0.88%.

A backscattered electron detector (BED) and Emission Scanning Electron Microscopy (JEOL JSM-7600F) to obtained SEM images were used. Tests were carried out to blade in leading and trailing edge (Figure 8) with field emission (show in Figure 9). In worn zone, 10 kV were applied and fourteen elements were found, such as chromium (Cr), nickel (Ni), molybdenum (Mo) and niobium (Nb). Percentages varied when evaluating a leading edge and another side, as shown Figure 9, but in analysis it was possible to identify the type of super alloy with 14 chemical elements in its composition.

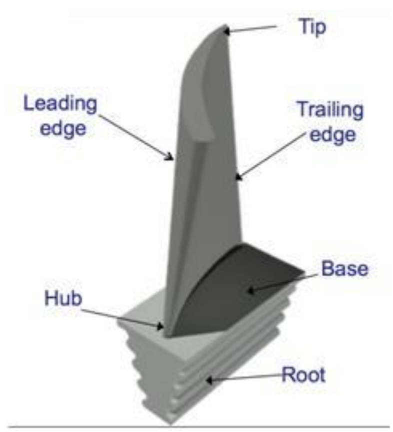


*Figure (8). Parts of blade: leading edge, trailing edge, root, base and hub.*

Preprints (www.preprints.org) | NOT PEER-REVIEWED | Posted: 18 January 2021 doi:10.20944/preprints202101.0350.v1


*Figure (9). BED and Emission Scanning Electron Microscopy test.*

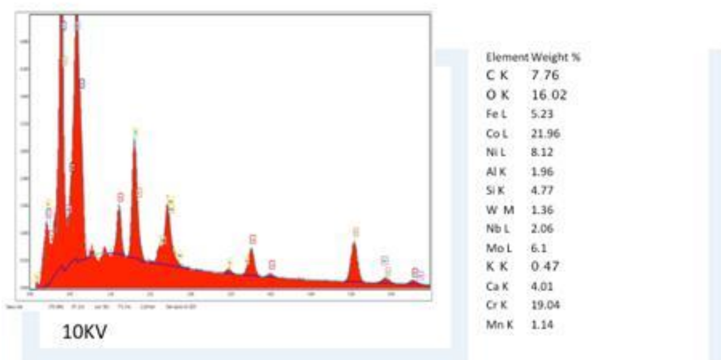


*Figure (10). Chemical analysis in a leading edge (chemical elements and EDS graph).*

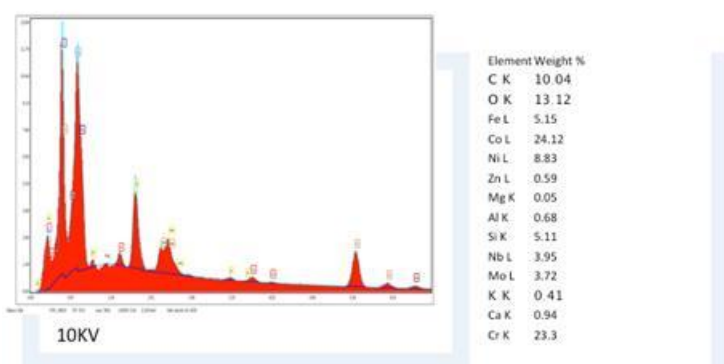


*Figure (11). Chemical analysis in trailing edge 8 chemical elements and EDS graph.*

Elements such as cobalt (Co), nickel (Ni), niobium (Nb) and molybdenum (Mo), with exception of Ni, these elements and weight percentages are close to martensitic stainless steel compositions [9].

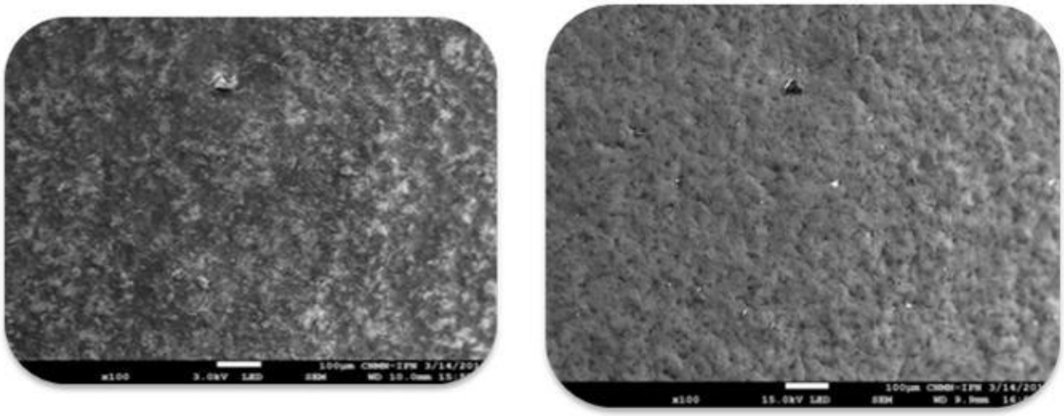

Leading edge Emission Scanning Electron Microscope

Trailing edge Emission Scanning Electron Microscope test.

*Figure (12). Worn region with 3KV and 15 KV (JEOL JSM-7600 SEM).*

3KV

| Element | Weight % | Atomic % |
|---|---|---|
| C K | 10.23 | 29.32 |
| O K | 8.95 | 19.25 |
| Al K | 2.71 | 3.45 |
| Si K | 2.82 | 3.46 |
| Nb L | 1.93 | 0.72 |
| Mo L | 1.83 | 0.66 |
| Cr K | 15.62 | 10.34 |
| Fe K | 3.07 | 1.9 |
| Co K | 35.15 | 20.53 |
| Ni K | 17.68 | 10.37 |

15KV

| Element | Weight % | Atomic % |
|---|---|---|
| C K | 8.46 | 25.22 |
| O K | 9.59 | 21.47 |
| Al K | 2.84 | 3.76 |
| Si K | 1.87 | 2.38 |
| K K | 0.04 | 0.03 |
| Ca K | 0.15 | 0.13 |
| Ti K | 0.34 | 0.25 |
| Cr K | 15.56 | 10.71 |
| Mn K | 0.98 | 0.64 |
| Fe K | 3.09 | 1.98 |
| Co K | 35.06 | 21.3 |
| Ni K | 17.75 | 10.83 |
| W L | 1.79 | 0.35 |
| Nb K | 0.38 | 0.15 |
| Mo K | 2.11 | 0.79 |

*Figure (13). Worn region with 3 KV and 15 KV (JEOL JSM-7600 SEM).*

In worn regions with 3KV and 15 KV (Figure 12) showed different elements than those observed in worn surface. In zones 1 and 2 (Figure 13), new chemical elements appeared in EDS analysis such as carbon (C), oxygen (O), aluminium (Al), silicon (Si), niobium (Ni), molybdenum (Mo), chromium (Cr), iron (Fe), cobalt (Co) and nickel (Ni) and when applying 15 KV new chemical elements appeared in EDS analysis such as carbon (C), oxygen (O), aluminium (Al), silicon (Si), potassium (K), calcium (Ca), titanium (Ti) chromium (Cr), manganese (Mn), iron (Fe), cobalt (Co), nickel (Ni), Tungsten (W), niobium (Ni) and molybdenum (Mo), which could be due to introduced particles (contaminants) travelling in air intake or from hot corrosion (accelerated oxidation damage) due to corrosive deposits. There is evidence of aluminium,

*Preprints* (www.preprints.org) | NOT PEER-REVIEWED | Posted: 18 January 2021 doi:10.20944/preprints202101.0350.v1

chromium and iron oxides in this region [12–13].

## 3. Scanning Electron Microscopy Analysis

In this phase of scanning, two techniques to preparation of the sample was used, first one analysis in trailing edge (Figure 14) and then leading edge of the piece (Figure 16), which are shown below:

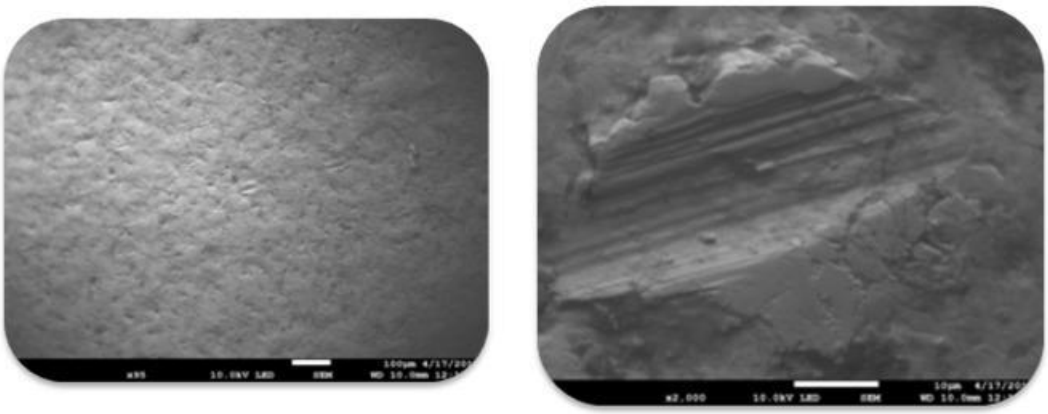

Irregular identation in leading edge. Identation with material piled-up.

*Fig. (14). Irregular indentation and material piled-up (trailing edge).*

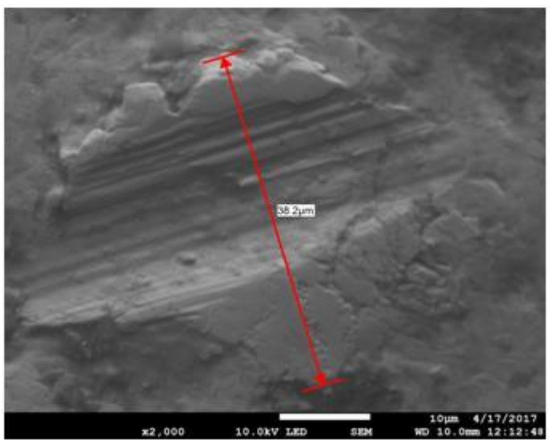


*Figure (15). Cavity around 38.2 µm*

*Preprints* (www.preprints.org) | NOT PEER-REVIEWED | Posted: 18 January 2021 doi:10.20944/preprints202101.0350.v1

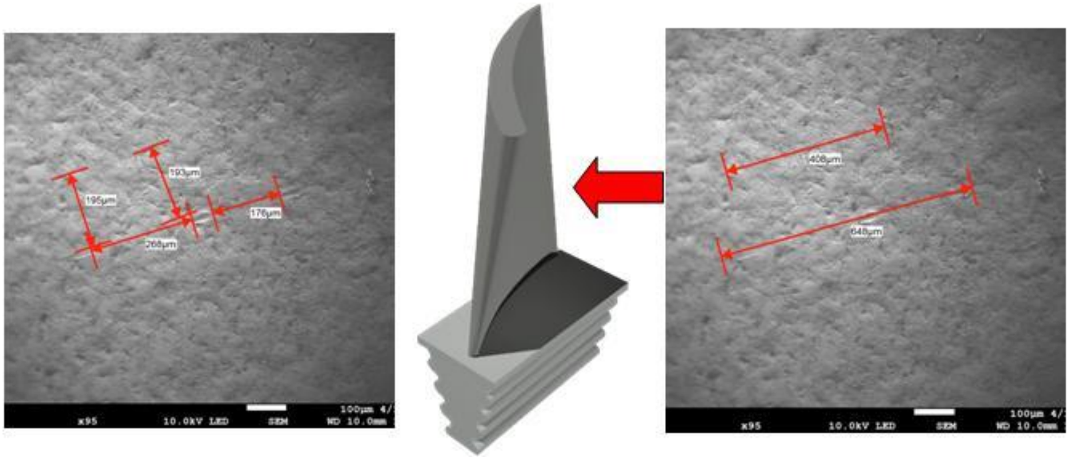


*Figure (16). Trailing edge (Emission Scanning Electron Microscopy test).*

Figure 16 in trailing edge, present irregular indentations were identified on surfaces around 176–268 µm length with material piled-up (lips) at sides and cavity around 38.2 µm (see Figure 15), the result of subsequent particle impacts, which caused detachment of lips with trajectory around 408–648 µm.

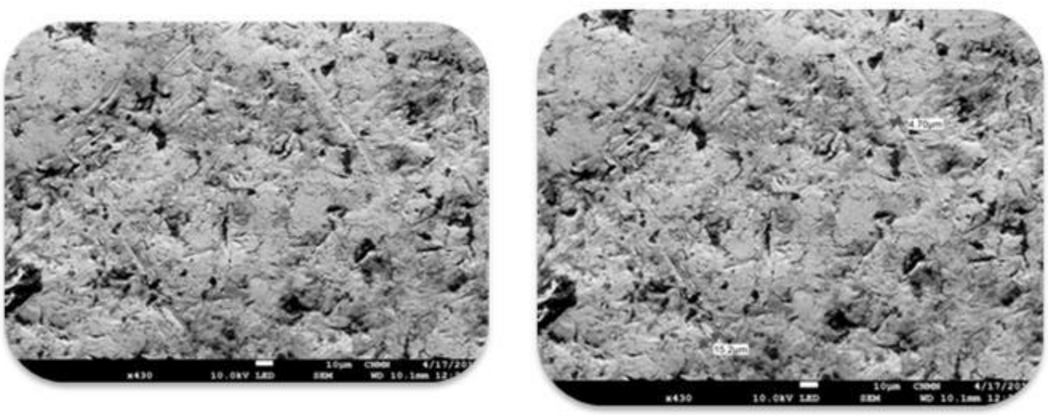

Large craters and grove (ploughing action) in trailing edge.

Ploughing action with material piled-up.

*Figure (17). Craters, grove and piled-up material (leading edge).*

 doi:10.20944/preprints202101.0350.v1

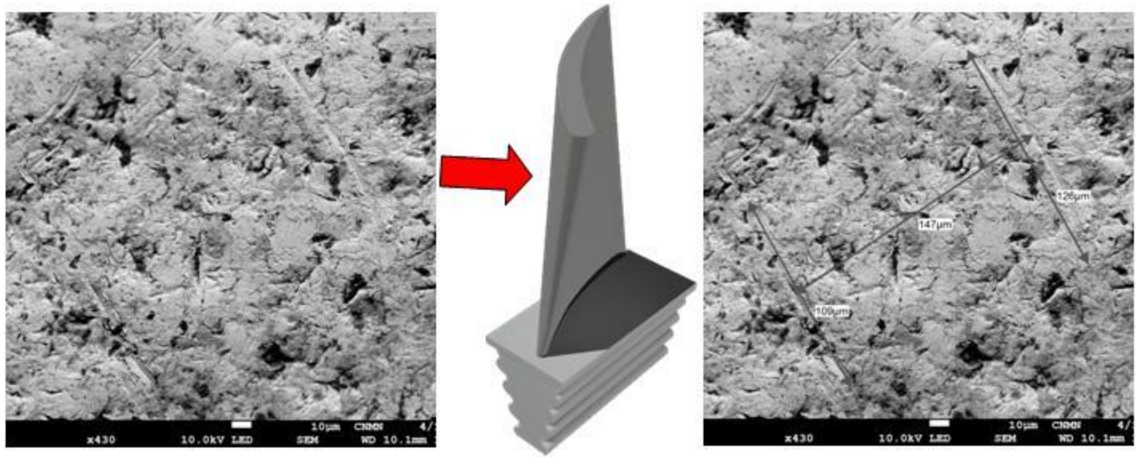

*Figure (18). Leading edge (Emission Scanning Electron Microscopy test).*

Images in Figures 17 and 18 in leading edge, which are characterized by large craters and grooves (ploughing action) of around 125–150 μm length with material piled-up (lips) at sides around 4.7–15.2 μm length and in front of cavities, which is common in solid particle erosion, as specimens are impacted at oblique incident angles (α ≤ 45°) [14].

## 4. Conclusions

In this paper a methodology was developed to carry out analysis of damage caused by wear of blades of axial compressor on a gas turbine. Different types of analysis were carried out in trailing edge and leading edge of blade, where in the Emission Scanning Electron Microscopy analysis it was obtained that blades are manufactured from a chrome-based superalloy with chemical elements such as Co, Cr, Ni, Fe, C, Nb and Mo, likewise analysis showed degradation of surfaces in areas of higher air pressure mixed with particles.

In microstructural tests, wear mechanisms characterized by large craters and grooves were identified, wear remains incorporated in surfaces of zones, and mechanisms were presented such as corrosion damage, irregular cavities, wear debris, flattened foreign particles on surface and parallel grooves showing the trajectory of solid particle impacted on blade during its operation.

Finally, this study shows the kind of damage caused by wear in axial compressor's blades on a gas turbine with some evidence of a witch corrosion and irregular scratches similar to plowing action, was observed. These are the points in which failures take place.

## 5. Author Contributions

Contributor Roles Taxonomy (CRediT)

| | **Authors** | | | | | |
|---|---|---|---|---|---|---|
| **Contribution type** | L.Y. Villagrán-Villegas | M. Patiño-Ortiz | L. H. Hernández-Gómez | J.A. Del Ángel-Ramos | J.C. Anzelmetti-Zaragoza | J.J. García-Mejía |
| Conceptualization | X | X | X | X | | |
| Data curation | X | X | X | X | X | X |
| Formal analysis | X | X | X | | | |
| Funding acquisition | X | X | X | X | X | X |
| Investigation | X | X | X | X | X | X |
| Methodology | X | X | X | | | |
| Project administration | X | | | | | |
| Resources | X | X | X | | | X |
| Software | - | - | - | - | - | - |
| Supervision | X | X | | X | | |
| Validation | X | X | X | X | X | X |
| Visualization | X | X | X | | | |
| Writing - original draft | X | X | X | X | X | X |
| Writing - review & editing | X | X | X | X | X | X |

## 6. References

[1] Tabakoff, H. S. (1998). Blade Deterioration in a Gas Turbine Engine. (G. science, Ed.) International Journal of Rotating Machinery, 4 (4), p. 233-241.

[2] Pettit, F. S., & Goward, G. W. (1981). High temperature corrosion and use of coatings for protection. Metallurgical Treatises, 1, p. 603-619.

[3] Hutchings, I. (2003). Tribology (Vol. 1). (B. Heinemann, Ed.) London, London, UK: Elsevier Science.

[4] Kurz. (2014). Gas turbine degradation. Turbomachinery Laboratory, 1 (1), p. 36.

[5] NageswaraRao, M. (2011). Materials for Gas Turbines – An Overview, Advances in Gas Turbine Technology.Intech Europe, University Campus STePRi. Rijeka: Intech.

Preprints (www.preprints.org) | NOT PEER-REVIEWED | Posted: 18 January 2021 doi:10.20944/preprints202101.0350.v1

[6] Shilke, P. W. (2004). Advanced Gas Turbine Materials and Coatings. (Ge, Ed.) Ge Power, 1 (p. 356).

[7] Solar Turbines A Caterpillar Company. (2007). Curso de operación y mantenimiento rutinario (Vol. 1). San Diego, C.A., USA: Solar Turbines Incorporated.

[8] Giampaolo, A. (2006). Gas Turbine Handbook; Principles and practices (3a. ed., Vol. 1). (CRC, Ed.) BR, Florida, USA: The Fairmont press.

[9] Romero CA, Campos-Amezcua A. (2007). Numerical investigation of the solid particle erosion rate in a steam turbine nozzle. Appl. ThermEng

[10] Mann BS. (1999). Solid-particle erosion and protective layers for steam turbine blading. Wear; 224: p. 8–12.

[11] Totten, G. E., & Liang, H. (2004). Mechanical Tribology. (Dekker, Ed.) Seattle, Washington, USA: Marcel Dekker Inc.

[12] N. Eliaz, G. Shemesh, R.M. Latanision (2002). Hot corrosion in gas turbine components, Eng. Fail. Anal. 9 p. 31–43.

[13] S. Kumari, D.V.V. Satyanarayana, M. Srinivas, (2014). Failure analysis of gas turbine rotor blades, Eng. Fail. Anal. 45, p. 234–244.

[14] T. Singh, S.N. Tiwari, G. Sundararajan (1991). Room temperature erosion behaviour of 304, 316 and 410 stainless steels, Wear 145, p. 77–100.

[15] R. Mendriky, Determination of measurement of accuracy of optical 3D scanner. Journal (Vol.1.) (2016), p. 1565-1572.

[16] Losertová, M. (2014). Advanced materials (Vol. 1). (VSB, Ed.) Ostrava: VSB.